Check for updates

ChemMedChem

Research Article
doi.org/10.1002/cmdc.202200549

Chemistry Europe
European Chemical Societies Publishing

www.chemmedchem.org

Peptides Targeting RNA m^{6}A Methylations Influence the Viability of Cancer Cells

Rushdhi Rauff,[a] Sudeshi M. Abedeera,[a] Stefani Schmocker,[a] Jiale Xie,[a] and Sanjaya C. Abeysirigunawardena*[a]

N6-methyladenosine (m^{6}A) is the most abundant nucleotide modification observed in eukaryotic mRNA. Changes in m^{6}A levels in transcriptome are tightly correlated to expression levels of m^{6}A methyltransferases and demethylases. Abnormal expression levels of methyltransferases and demethylases are observed in various diseases and health conditions such as cancer, male infertility, and obesity. This research explores the efficacy of m^{6}A-modified RNA as an anticancer drug target. We discovered a 12-mer peptide that binds specifically to m^{6}A-modified RNA using phage display experiments. Our fluorescence-based assays illustrate the selected peptide binds to methylated RNA with lower micromolar affinity and inhibit the binding of protein FTO, a demethylase enzyme specific to m^{6}A modification. When cancer cell lines were treated with mtp1, it led to an increase in m^{6}A levels and a decrease in cell viability. Hence our results illustrate the potential of mtp1 to be developed as a drug for cancer.

Cancer is the second most cause of death in the USA after heart disease.[1] In 2020, nearly 19.3 million new cancer cases and 10 million deaths due to cancer were recorded worldwide.[2] In Europe, over 1.2 million cancer-related deaths are expected in 2022 alone.[3] Numerous chemotherapeutic approaches to combat cancer have been used together with surgery, radiotherapy, and immunotherapy.[4–6] In response to off-target binding and high cytotoxicity of widely used chemotherapeutics, developing highly effective and efficient drugs that bind to novel drug targets is essential.[7,8]

Nucleotide modification levels in mRNA change under various cellular stresses.[9] Such changes in mRNA nucleotide modification levels are also associated with many human diseases and conditions. For example, N6-methyladenosine (m^{6}A) levels in mRNA decrease in the presence of lung cancer, glioblastoma, breast cancer, and β cells extracted from diabetes patients, whereas elevated m^{6}A levels are observed in colorectal cancer, pancreatic cancer, and acute myeloid leukemia. In parallel to the changes in m^{6}A levels, expression levels of m^{6}A methyltransferases (writers) and demethylases (erasers) also change appropriately in cancer cell lines tested.[10–12] N6-methylations in RNA are also recognized by m^{6}A reader proteins leading to the regulation of cellular protein levels.[13] We find targeting m^{6}A-modified mRNA a feasible approach to inhibit the binding of methyl readers and erasers, thus altering the expression of many oncoproteins and tumor suppressor proteins.

Here we use phage display, a directed evolution method, to identify peptides that bind to m^{6}A-modified regions in RNA and block the binding of m^{6}A-recognizing proteins. Phage display has been used to discover peptide-based therapeutic agents approved by the FDA, such as Raxibacumab and Romiplostim.[14,15] In addition, many potential peptide chemotherapeutics currently in different drug development phases are discovered through the phage display method.[16–18] Interestingly, all peptide-based cancer drug candidates target proteins. However, many previous studies illustrate that phage display can be successfully used to discover RNA-binding peptides that can be used as therapeutics.[19–23]

The target RNA used in phage display has the most abundant m^{6}A modified sequence (GGm^{6}AC) observed in mRNA. A random RNA sequence is added to the 5′-end of the GGm^{6}ACA sequence to keep the targeted sequence away from the solid support. The 5′-end of the target RNA is conjugated to a biotin moiety that enables the target RNA to be immobilized in the streptavidin-coated magnetic beads (NEB labs). Immobilized target RNAs were then incubated with Ph.D.-12 M13 phage library (NEB labs). Unbound phages were removed by washing. The bound phages were then eluted and used in the next biopanning cycle, followed by amplification. The stringency of the washing was increased gradually in each subsequent biopanning cycle by 1) increasing detergent concentration in washing buffers, 2) increasing the number of washings, and 3) adding various competitor RNAs. In the 4th cycle, DNA from individual phage colonies was extracted and sequenced to determine the randomized 12-mer peptide fused to the pIII coat protein. Approximately 23% of the peptides selected against the methylated RNA target (MT-RNA) had DGDWDAWTRETS (mtp1) amino acid sequence (Figure 1a). Although all the other enriched peptides had similar peptide sequences, they were less abundant (<8%). RNA-binding

[a] R. Rauff, S. M. Abedeera, S. Schmocker, J. Xie, Dr. S. C. Abeysirigunawardena
Department of Chemistry and Biochemistry
Kent State University
1175 Risman Drive, Kent OH 44242 (USA)
E-mail: sabeysir@kent.edu

Supporting information for this article is available on the WWW under https://doi.org/10.1002/cmdc.202200549

© 2022 The Authors. ChemMedChem published by Wiley-VCH GmbH. This is an open access article under the terms of the Creative Commons Attribution Non-Commercial License, which permits use, distribution and reproduction in any medium, provided the original work is properly cited and is not used for commercial purposes.

© 2022 The Authors. ChemMedChem published by Wiley-VCH GmbH

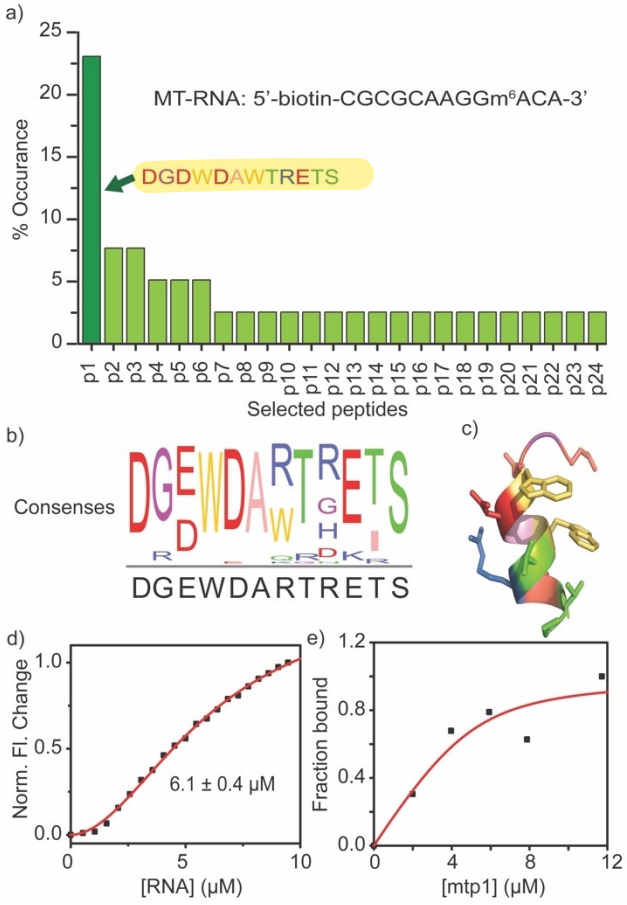

Figure 1. The most enriched peptide in phage display against m6 A-modified RNA target, mtp1 binds tightly to RNA. a) Percentage occurrence of peptides after four cycles of biopanning is shown. b) sequence logo for all the selected peptides illustrates high sequences conservation among the enriched peptides. c) The structure of the most abundant peptide (mtp1) predicted by the PEPFOLD3 algorithm. The mtp1 peptide is composed of positively charged (red), negatively charged (blue), and aromatic (lilac) amino acid residues. d) RNA titration curve (0–10 μM) constructed using tryptophan fluorescence change for mtp1 peptide. e) Peptide titration curve (0–12 μM). The fraction bound was calculated using circular dichroism change of RNA (276–280 nm). All titrations were performed in triplicate to ensure reproducibility.

proteins typically contain positively charged amino acid residues clustered around the RNA binding site due to their ability to form ionic interactions with the negatively charged phosphate backbone of RNAs. However, these ionic interactions between RNA and proteins are most likely non-specific. Interestingly, the most abundant peptide carries only one positively charged amino acid residue; nevertheless, three negatively charged aspartic acid residues at positions 1, 3, and 5 in the dodecamer peptide sequence. Most of the peptides selected against the methylated target illustrated a sequence similarity to mtp1. Amino acids D1, W4, D5, A6, and S12 are nearly 100% conserved among all observed sequences (Figure 1b). In addition, tryptophan at position 7 of the peptide is also highly conserved. These highly conserved residues in the mtp1 can play a role in forming stable RNA-peptide interactions.[24–26]

A stronger binding affinity of the drug molecules to their respective target is critical to achieving a higher drug efficacy. Previous studies illustrate that the equilibrium dissociation constants (Kd) of RNA-short peptide complexes range from 0.5 μM to 10 μM. A tryptophan fluorescence assay was performed to determine the ability of mtp1 to bind to RNA with micromolar affinity. A 55% decrease in tryptophan fluorescence with the addition of MT-RNA suggests that RNA binds close to the two tryptophan residues. A K_d of 6.1 ± 0.3 μM for mtp1-RNA complex was obtained by least- square fitting of RNA titration curves to Hill equation (Figure 1d). Surprisingly, the Hill coefficient was 1.9 ± 0.1, suggesting two highly corporative RNA binding events to a single peptide. Two RNA binding sites with equal affinity are unlikely to be available in a single peptide molecule. However, the two tryptophan residues on the peptide can act as two binding sites with an equal affinity that can potentially mimic two RNA strands binding to a single peptide strand. The binding of mtp1 to the MT-RNA strand was further analyzed by circular dichroism spectroscopy. The change in circular dichroism at 276 and 280 nm wavelength was measured as mtp1 (0 −12 μM) was titrated onto RNA. The least-square fitting of these peptide titration curves to the quadratic equation yields a K_d of 0.42 ± 0.09 μM for the RNA-peptide complex (Figure 1e, S1). In addition, the total RNA concentration obtained from the quadratic fits is similar to the [mtp1] at saturation suggesting approximately a 1:1 stoichiometry between RNA and peptide. Both binding assays illustrate similar low micromolar binding affinity for mtp1 to methylated RNA comparable to many RNA-binding short peptides discovered previously.[19,22,23] The 14-fold higher K_d observed from fluorometric assay can be due to the averaging of changes from two tryptophan residues in the peptide. Control binding experiments performed using the RNA with the same sequence (Figure S2) illustrates that mtp1 can bind to unmethylated RNA but with a significantly higher K_d than for its methylated counterpart.

Many small-molecular inhibitors of epitranscriptomic regulation discovered over the years bind to proteins involved in the regulation, such as m^6A eraser proteins. It is necessary for the peptide to inhibit protein binding to methylated RNA to influence epitranscriptomic regulation. A FRET-based competitive binding assay was used to evaluate the ability of the mtp1 peptides to inhibit the binding of fat mass obesity associated protein (FTO), an α-ketoglutarate-dependent dioxygenase that demethylates m^6A nucleotides (Figure 2a). Using FRET-based titrations of fluorescently labeled FTO protein (FTO-Cy5) onto MT-RNA (5 nM) labeled with the FRET donor Cy3 (Cy3-MT-RNA), a K_d of 3.8 ± 0.7 nM for FTO-RNA complex was obtained (Figure 2b). The addition of high stoichiometric excess of FTO (20 nM) to MT-RNA (5 nM) gave rise to a 0.081 FRET efficiency. However, when MT-RNA is preincubated with mtp1 before the addition of saturating concentration of FTO, the FRET efficiency decreases with increasing peptide concentration (0–10 μM), suggesting the ability of the peptide to inhibit FTO binding to RNA (Figure 2c). The K_I of mtp1 for FTO binding to m^6A modified RNA (0.47 ± 0.05 μM) falls in the range of other known FTO inhibitors (0.06 to 105.6 μM).[27,28]

© 2022 The Authors. ChemMedChem published by Wiley-VCH GmbH

18607187, 2023, 4, Downloaded from https://chemistry-europe.onlinelibrary.wiley.com/doi/10.1002/cmdc.202200549 by Indraprastha Institute Of Information Technology, Delhi, Wiley Online Library on [13/01/2024]. See the Terms and Conditions (https://onlinelibrary.wiley.com/terms-and-conditions) on Wiley Online Library for rules of use; OA articles are governed by the applicable Creative Commons License

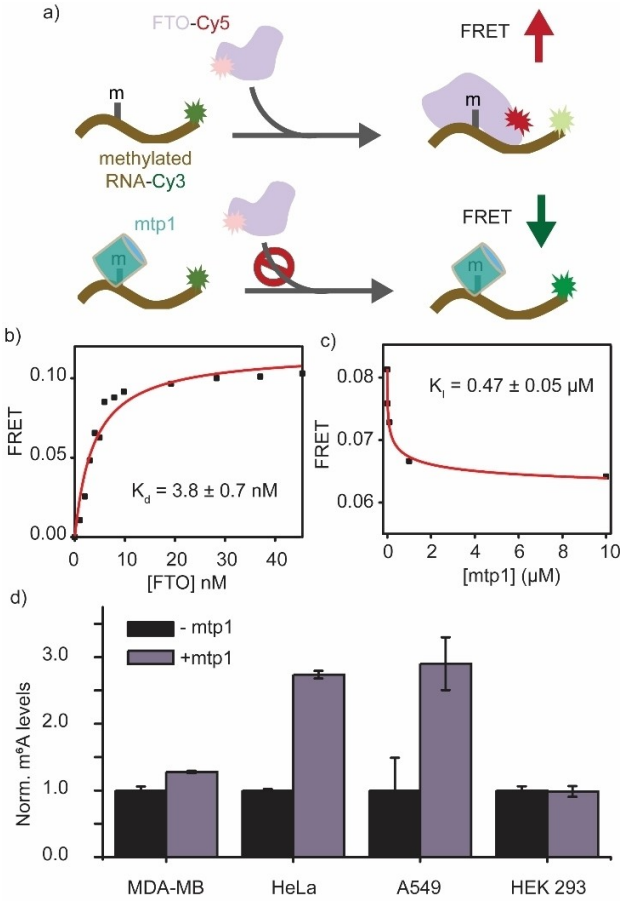

Figure 2. The mtp1 peptide inhibits the binding and demethylase activity of FTO. a) Schematic representation of FTO binding inhibition assay. b) FRET between cyanine dyes on RNA and FTO plotted against FTO concentrations. FTO titration curves were fitted quadratic equation to determine the K_d for the FTO-RNA complex. c) Changes in FRET for FTO-RNA complexes with increasing mtp1 concentration are shown. d) m^6A levels in total RNA increase in the presence of mtp1. Error bars represent the standard deviation of biological triplicates.

In certain cancer types, FTO levels are upregulated, causing an increase in FTO-mRNA complexes followed by a decrease in mRNA methylations. Decreased levels of methylation in proto-oncogenes and tumor suppressor genes will regulate their expression and thus leading to increased oncogenicity of tumors. Inhibiting FTO binding to its target RNA will increase mRNA methylation levels and decrease oncogenicity. We hypothesized that mtp1 could decrease the activity of FTO and thus increase the level of methylations in cancer cells. An ELISA-based method from Epigentek (EpiQuik m^6A RNA Methylation Quantification Kit) was used to test total RNA m^6A levels in several cancer cell lines. The m^6A levels of the treated (10 μM mtp1) cells were compared with that of untreated cells. A significant increase in the m^6A levels was observed for all cancer cell lines tested. Lung cancer (A549) and cervical cancer (HeLa) cells showed the highest increase in m^6A levels (2.7- and 2.9-fold increase, respectively) with the addition of 10 μM of mtp1 (Figure 2d). Surprisingly, however, a significant change in m^6A levels upon treatment of mtp1 (10 μM) was not observed in the non-cancerous HEK293 cell line.

Since mtp1 binds to methylated RNA, we anticipated a decrease in the viability of cancerous cells upon adding mtp1. Several cancer cell lines were transfected with mtp1 (TransIT–X2 Dynamic Delivery System, Mirus Bio). Cells were grown for another 24 hours after transfection and measured cell viability by MTS assay. Treatment of MDA-MB 231, HeLa, and A549 with 10 μM of mtp1 illustrated a 33.6%, 30.2%, and 17.4% decrease in cell viability, respectively (Figure 3a, Figure S3). A significant drop in the cell viability was not observed upon treatment of a control peptide (10 μM) that was selected against a 16S h34 rRNA target using phage display (Figure 3c).[19] This observation emphasizes the ability of mtp1 to influence the viability of cancer cells. HEK 293 cells were treated with 10 μM mtp1 peptide to test the viability of non-cancerous cells. Surprisingly, the cell viability increased by 4.5%, suggesting that mtp1 is not cytotoxic for non-cancerous cells (Figure 3a). The IC_{50} for MDA-MB 231 cells that exhibited the highest drop in cell viability was found to be 7.7 ± 0.3 μM (Figure 3c). Surprisingly, the cell viability decreased to only ~40% even after adding 12 μM of mtp1 (Figure 3c). The inability of the mtp1 to completely abolish cell viability can be attributed to the limitations in mtp1 transfection. MDA-MB 231 cells were treated with mtp1 (10 μM) using twice the amount of transfection reagent (6 μL) to test if the transfection reagent was the limiting factor. Doubling the transfection reagent almost decreased the cell viability by half, clearly suggesting that the transfection reagent acts as the limiting factor in cell viability.

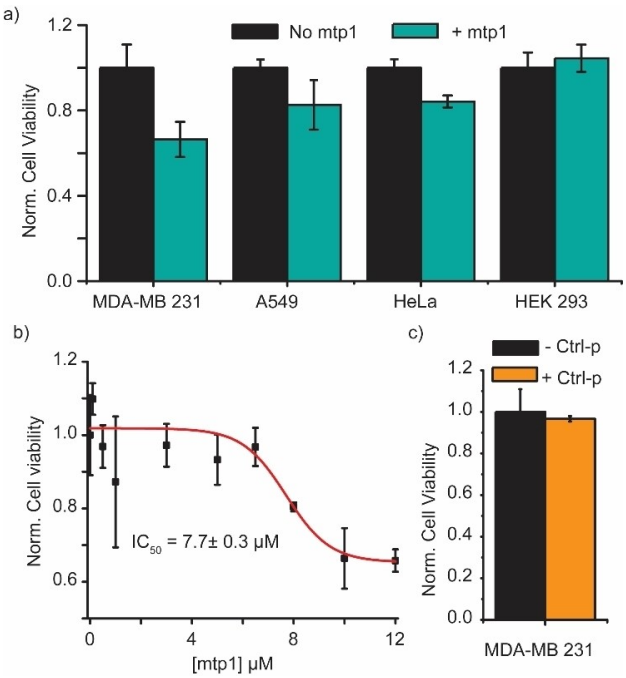

Figure 3. The mtp1 peptide decreases cancer cell viability. a) The decrease in viability of various cancer cells upon transfection of mtp1 is shown. The standard deviation of three biological replicates is shown as error bars. b) The IC_{50} of mtp1 for MDA-MB 231 cells. c) Viability of MDA-MB cells upon transfection of a control peptide is shown.

© 2022 The Authors. ChemMedChem published by Wiley-VCH GmbH

18607187, 2023, 4, Downloaded from https://chemistry-europe.onlinelibrary.wiley.com/doi/10.1002/cmdc.202200549 by Indraprastha Institute Of Information Technology, Delhi, Wiley Online Library on [13/01/2024]. See the Terms and Conditions (https://onlinelibrary.wiley.com/terms-and-conditions) on Wiley Online Library for rules of use; OA articles are governed by the applicable Creative Commons License

Due to the lack of cleft-like target sites that increase the specificity of drug binding, only a small fraction of proteins from the total human proteome can function as drug targets. Targeting mRNA is an excellent strategy to target undruggable proteins lacking cleft-like target sites.[29] This strategy will also enable simultaneous targeting of multiple oncoproteins. Previous efforts to target epitranscriptomic regulation are currently centered on FTO inhibition. FTO inhibitors that are analogs of its substrate, α-ketoglutarate, can also bind to enzymes such as α-ketoglutarate dehydrogenase found in the TCA cycle. Similarly, pyrimidine-like FTO inhibitors may bind to many nucleic acid binding proteins other than FTO. Unlike current FTO inhibitors, the ability of mtp1 to bind to methylated mRNA enables this peptide to work as a universal inhibitor of m^6A recognition. The 1.3- to 2.9-fold increase in the N6-methylation levels for mtp1 is comparable to a 1- to 3-fold increase in m^6A levels upon treating cells with various other small-molecular inhibitors of FTO.[27,31,32] In addition, mtp1 and other FTO inhibitors are found to have similar IC_{50}s. In conclusion, mtp1 binds with the m^6A modified RNAs, decreasing cancer cell viability. In addition, mtp1 was found to be less cytotoxic to non-cancerous cells. Developing a targeted delivery method that guides mtp1 to cancer cells will make mtp1 a successful chemotherapeutic agent similar to many FDA-approved peptide drugs against cancer, such as Carfilzomib and Lutathera.[33–35]

Acknowledgements

The authors thank the US National Institute of General Medical Sciences (NIGMS, grant number R15GM137291) for research funding.

Conflict of Interest

The authors declare no conflict of interest.

Data Availability Statement

The data that support the findings of this study are available from the corresponding author upon reasonable request.

Keywords: FTO · m^6A · phage display · peptide inhibitors · epitranscriptomics

[1] "Cancer Facts & Figures 2022| American Cancer Society," can be found under https://www.cancer.org/research/cancer-facts-statistics/all-cancer-facts-figures/cancer-facts-figures-2022.html, **n.d**.
[2] H. Sung, J. Ferlay, R. L. Siegel, M. Laversanne, I. Soerjomataram, A. Jemal, F. Bray, *Ca-Cancer J. Clin.* **2021**, *71*, 209–249.
[3] M. Dalmartello, C. La Vecchia, P. Bertuccio, P. Boffetta, F. Levi, E. Negri, M. Malvezzi, *Ann. Oncol.* **2022**, *33*, 330–339.
[4] B. Nordlinger, E. Van Cutsem, T. Gruenberger, B. Glimelius, G. Poston, P. Rougier, A. Sobrero, M. Ychou, *Ann. Oncol.* **2009**, *20*, 985–992.
[5] X. Ning, Y. Yu, S. Shao, R. Deng, J. Yu, X. Wang, X. She, D. Huang, X. Shen, W. Duan, J. Duan, H. Zhang, *Ann. Transl. Med.* **2021**, *9*, 1703.
[6] T. B. Brunner, *Best Pract. Res. Clin. Gastroenterol.* **2016**, *30*, 515–528.
[7] T. B. de Castria, E. M. K. da Silva, A. F. T. Gois, R. Riera, *Cochrane Database Syst. Rev.* **2013**, CD009256.
[8] M. L. C. Santos, B. B. de Brito, F. A. F. da Silva, A. C. dos S. Botelho, F. F. de Melo, *World J. Clin. Oncol.* **2020**, *11*, 190–204.
[9] B. S. Zhao, I. A. Roundtree, C. He, *Nat. Rev. Mol. Cell Biol.* **2017**, *18*, 31–42.
[10] D. Dai, H. Wang, L. Zhu, H. Jin, X. Wang, *Cell Death Dis.* **2018**, *9*, 124.
[11] R. Gao, M. Ye, B. Liu, M. Wei, D. Ma, K. Dong, *Front. Oncol.* **2021**, *11*, 679367.
[12] F. Bornaque, C. P. Delannoy, E. Courty, N. Rabhi, C. Carney, L. Rolland, M. Moreno, X. Gromada, C. Bourouh, P. Petit, E. Durand, F. Pattou, J. Kerr-Conte, P. Froguel, A. Bonnefond, F. Oger, J.-S. Annicotte, *Cells* **2022**, *11*, 291.
[13] S. Zaccara, R. J. Ries, S. R. Jaffrey, *Nat. Rev. Mol. Cell Biol.* **2019**, *20*, 608–624.
[14] A. E. Nixon, D. J. Sexton, R. C. Ladner, *mAbs* **2014**, *6*, 73–85.
[15] S. Mimmi, D. Maisano, I. Quinto, E. Iaccino, *Trends Pharmacol. Sci.* **2019**, *40*, 87–91.
[16] A. Wada, T. Terashima, S. Kageyama, T. Yoshida, M. Narita, A. Kawauchi, H. Kojima, *Mol. Ther. Oncolytics* **2019**, *12*, 138–146.
[17] P. E. Saw, E.-W. Song, *Protein Cell* **2019**, *10*, 787–807.
[18] C. Zhou, J. Kang, X. Wang, W. Wei, W. Jiang, *BMC Cancer* **2015**, *15*, 889.
[19] K. Gc, D. To, K. Jayalath, S. Abeysirigunawardena, *RSC Adv.* **2019**, *9*, 40268–40276.
[20] D. Koirala, A. Lewicka, Y. Koldobskaya, H. Huang, J. A. Piccirilli, *ACS Chem. Biol.* **2020**, *15*, 205–216.
[21] D. N. Dremann, C. S. Chow, *Bioorg. Med. Chem.* **2016**, *24*, 4486–4491.
[22] M. Kaur, C. N. Rupasinghe, E. Klosi, M. R. Spaller, C. S. Chow, *Bioorg. Med. Chem.* **2013**, *21*, 1240–1247.
[23] T. N. Lamichhane, N. D. Abeydeera, A.-C. E. Duc, P. R. Cunningham, C. S. Chow, *Molecules* **2011**, *16*, 1211–1239.
[24] F. Li, D. Zhao, J. Wu, Y. Shi, *Cell Res.* **2014**, *24*, 1490–1492.
[25] C. Xu, X. Wang, K. Liu, I. A. Roundtree, W. Tempel, Y. Li, Z. Lu, C. He, J. Min, *Nat. Chem. Biol.* **2014**, *10*, 927–929.
[26] T. Zhu, I. A. Roundtree, P. Wang, X. Wang, L. Wang, C. Sun, Y. Tian, J. Li, C. He, Y. Xu, *Cell Res.* **2014**, *24*, 1493–1496.
[27] Y. Huang, R. Su, Y. Sheng, L. Dong, Z. Dong, H. Xu, T. Ni, Z. S. Zhang, T. Zhang, C. Li, L. Han, Z. Zhu, F. Lian, J. Wei, Q. Deng, Y. Wang, M. Wunderlich, Z. Gao, G. Pan, D. Zhong, H. Zhou, N. Zhang, J. Gan, H. Jiang, J. C. Mulloy, Z. Qian, J. Chen, C.-G. Yang, *Cancer Cell* **2019**, *35*, 677–691.e10.
[28] M. Das, T. Yang, J. Dong, F. Prasetya, Y. Xie, K. H. Q. Wong, A. Cheong, E. C. Y. Woon, *Chem. Asian J.* **2018**, *13*, 2854–2867.
[29] K. D. Warner, C. E. Hajdin, K. M. Weeks, *Nat. Rev. Drug Discovery* **2018**, *17*, 547–558.
[30] G. Zheng, T. Cox, L. Tribbey, G. Z. Wang, P. Iacoban, M. E. Booher, G. J. Gabriel, L. Zhou, N. Bae, J. Rowles, C. He, M. J. Olsen, *ACS Chem. Neurosci.* **2014**, *5*, 658–665.
[31] S. Huff, S. K. Tiwari, G. M. Gonzalez, Y. Wang, T. M. Rana, *ACS Chem. Biol.* **2021**, *16*, 324–333.
[32] G. Xie, X.-N. Wu, Y. Ling, Y. Rui, D. Wu, J. Zhou, J. Li, S. Lin, Q. Peng, Z. Li, H. Wang, H.-B. Luo, *Acta Pharm. Sin. B* **2022**, *12*, 853–866.
[33] S. Marqus, E. Pirogova, T. J. Piva, *J. Biomed. Sci.* **2017**, *24*, 21.
[34] K. M. Kortuem, A. K. Stewart, *Blood* **2013**, *121*, 893–897.
[35] J. Underwood, G. Sturchio, S. Arnold, *Health Phys.* **2021**, *121*, 160–165.

Manuscript received: October 10, 2022
Revised manuscript received: December 13, 2022
Accepted manuscript online: December 25, 2022
Version of record online: January 23, 2023

© 2022 The Authors. ChemMedChem published by Wiley-VCH GmbH

18607187, 2023, 4, Downloaded from https://chemistry-europe.onlinelibrary.wiley.com/doi/10.1002/cmdc.202200549 by Indraprastha Institute Of Information Technology, Delhi, Wiley Online Library on [13/01/2024]. See the Terms and Conditions (https://onlinelibrary.wiley.com/terms-and-conditions) on Wiley Online Library for rules of use; OA articles are governed by the applicable Creative Commons License